Design for MOSIS Educational Program (Teaching)

T46TCA, T46TBZ

Project Title

PROJECT TITLE

Prepared by: B. Weather, S. Chen, S. Terry, B. J. Blalock, S. K. Islam

Institution: Department of Electrical and Computer Engineering,
University of Tennessee, 37996-2100

1. Objective

The objective of this project is to design and implement a bioluminescent micro-luminometer with on-chip temperature sensor.

2. Overview

2.1. Micro-luminometer system

The micro-luminometer system is designed to create a variable frequency output. The frequency is dependent upon and changes with the amount of incident light on the system's photo-detector. Figure 1 shows the system diagram of the micro-luminometer.

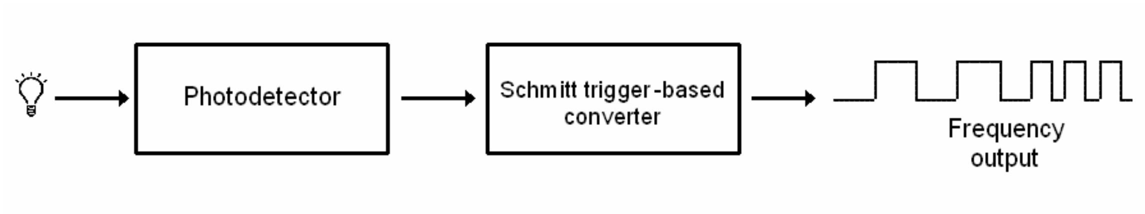

Figure 1 Micro-luminometer System

2.2. Temperature sensor

The temperature sensor is designed to generate two different types of output: current output in which the output current is proportional to the temperature and frequency output in which the output frequency indicates the temperature. Figure 2 shows the system diagram of the sensor.

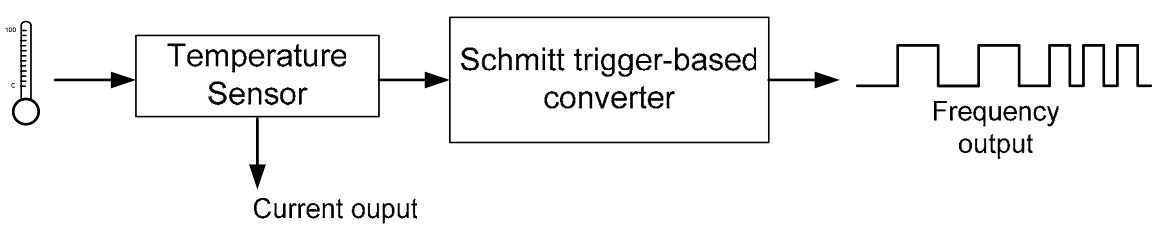

Figure 2 Temperature sensor

3. Design & Simulations

3.1. Design steps

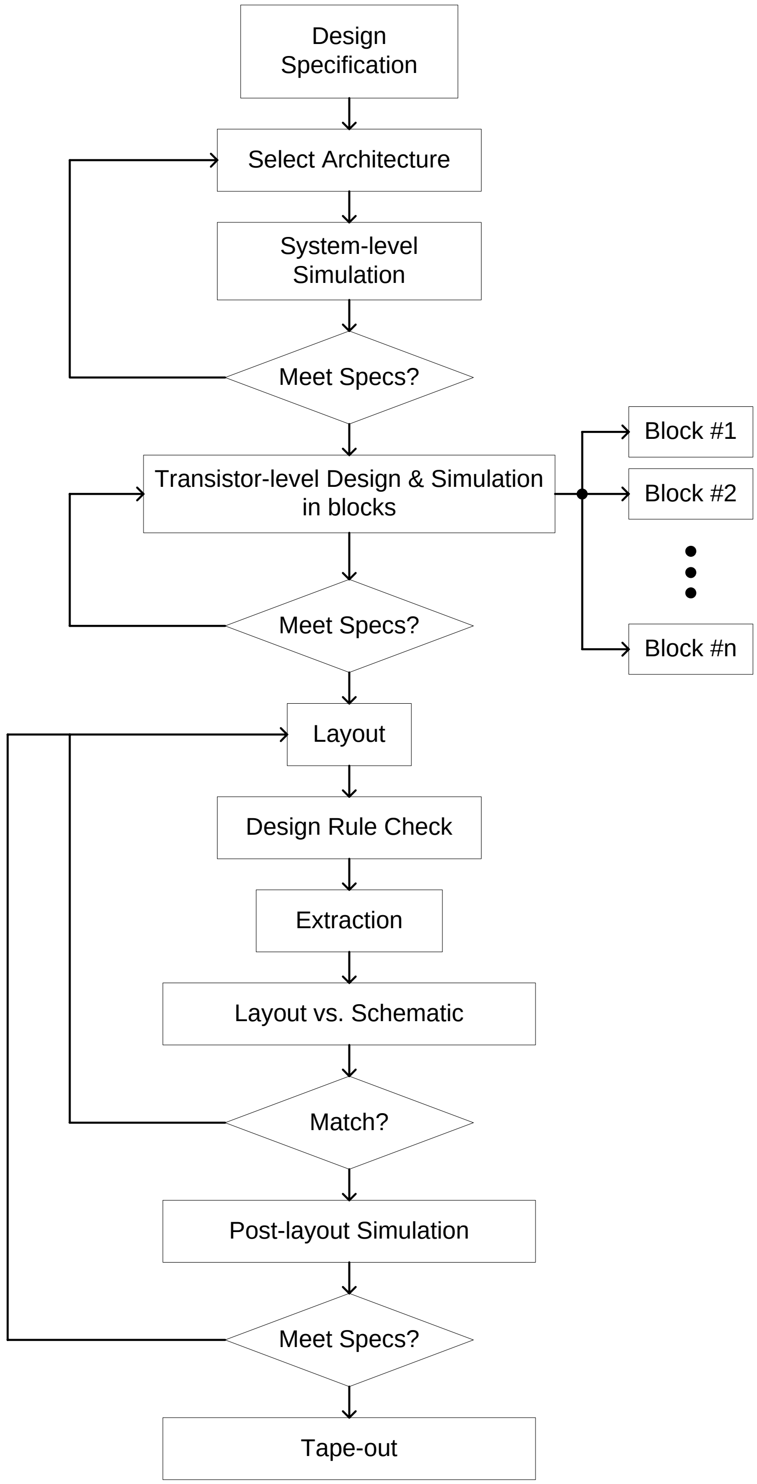

Figure 3 Flowchart of design steps

3.2. Bioluminescent Micro-luminometer System

The micro-luminometer schematic is shown in Figure 4. The incident light on the photodiode creates current that is converted into a frequency.

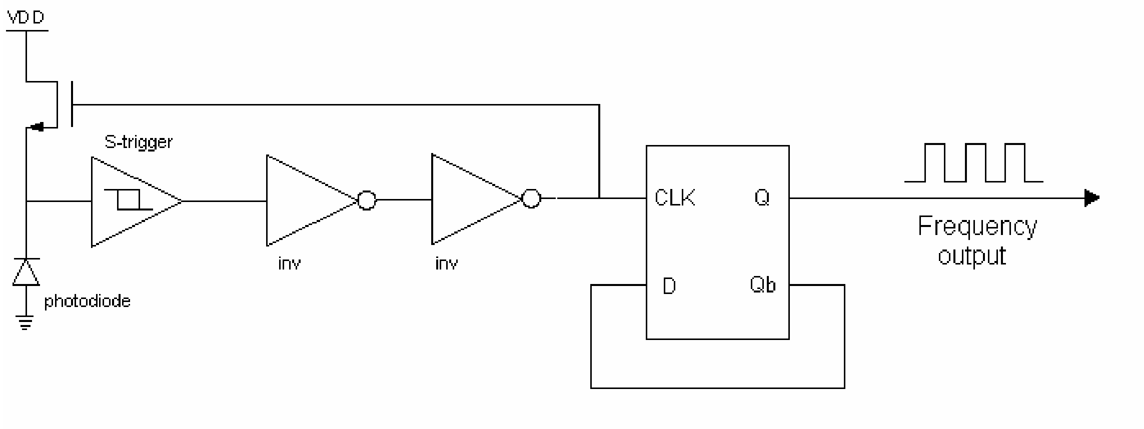

Figure 4 Micro-luminometer System Schematic

The micro-luminometer's primary use is for bacteria based bioluminescent systems which produce very low intensity light. The frequency, given by

$$f = \frac{I}{Q} = \frac{I}{CV},$$

Is proportional to the current, which is proportional to the population of the bacteria colony. The Schmitt trigger schematic is shown in Figure 9.

3.3. Temperature sensor

3.3.1. Current-output sensor

The schematic of the current-output sensor [1] is shown in Figure 5. The output current can be written as

$$I = k_{m1}\left(\frac{W}{L}\right)_1 \frac{\left(V + V_{T2} - V_{T1}\right)^2}{\left(1 - \sqrt{m}\right)^2}$$

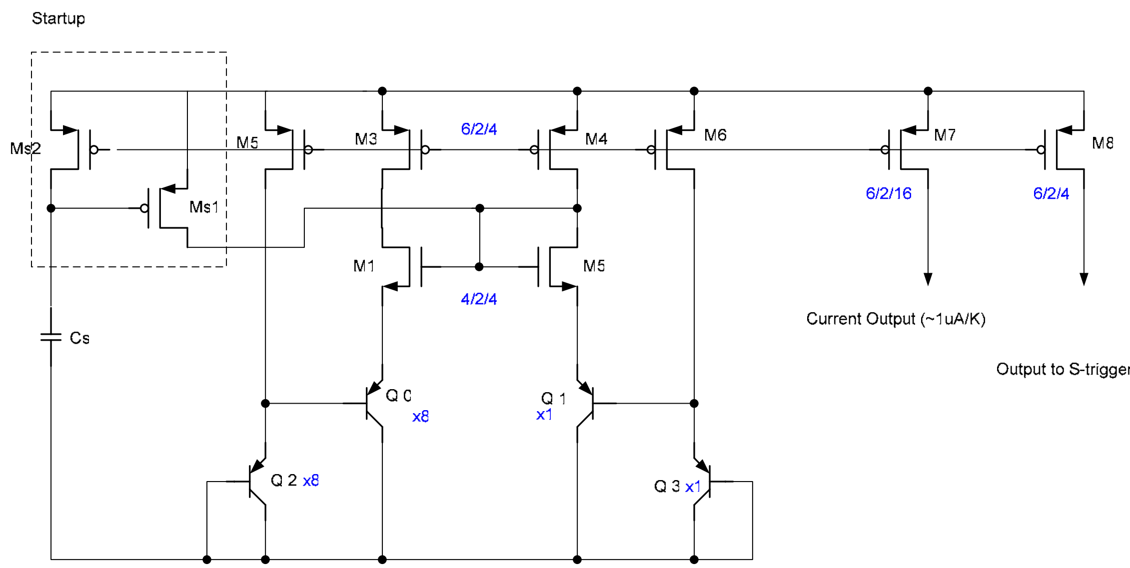

Figure 5 Current output sensor schematic

Since the mobility exponent is a process-dependent term and is often close to 1.5, the output current has a temperature exponent of around 0.5 after compensating with the PTAT voltage established by the Q0-3. Although the temperature exponent of the output current is not exactly 1, the output current has a very linear characteristic across a wide temperature range. Compared with using resistor to establish the current (e.g. beta-multiplier), using this approach the output current is less affected by the process variation. Simulation shows that the change of output current per degree change in temperature is 0.143 µA, shown in Figure 6.

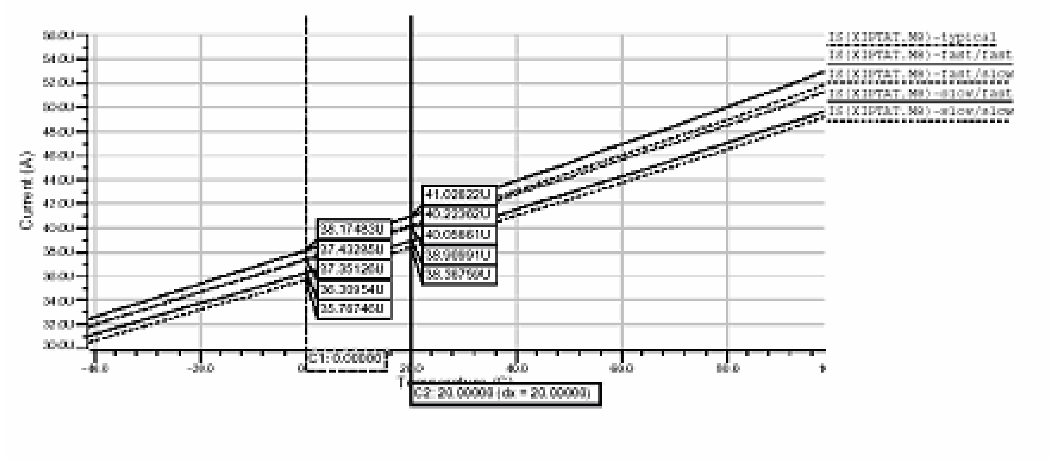

Figure 6 Current output versus temperature

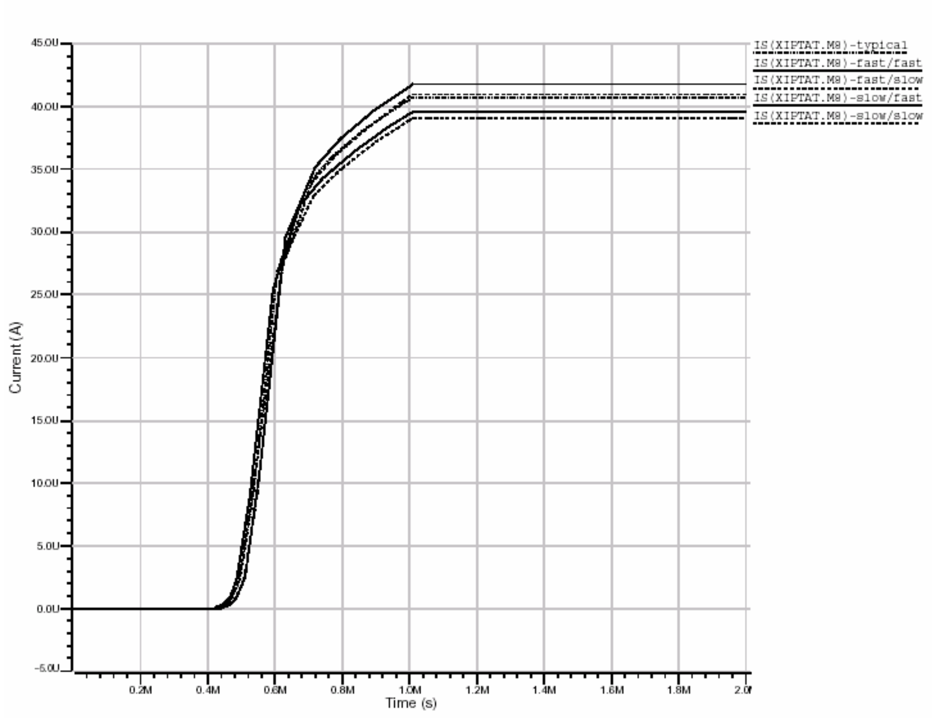

Figure 7 Startup simulation at different process corners

Just like all the self-biasing circuits, the start-up behavior is carefully examined to guarantee its start-up at different process corners. Figure 7 shows that the circuit will start up at all the process extremes, including typical, slow-slow, fast-fast, fast-slow, and slow-fast.

3.3.2. Frequency-output sensor

In order to generate more convenient temperature readings, the output current is converted into frequency. Figure 8 shows the schematic of a Schmitt trigger-based converter.

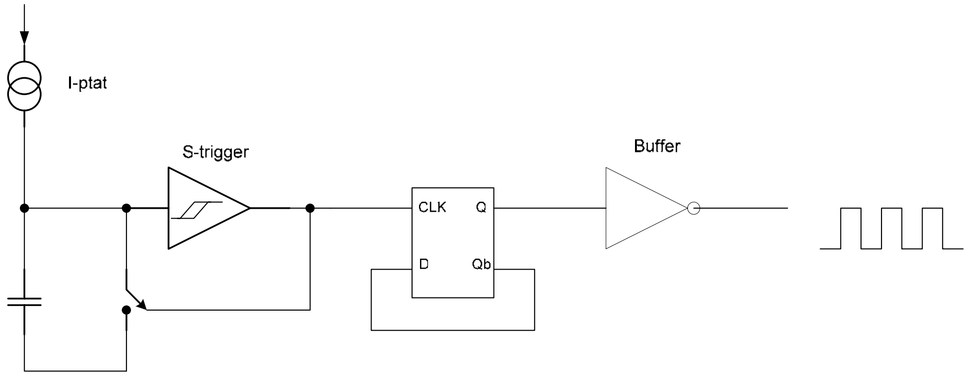

Figure 8 Frequency output schematic

Since the time it takes the input current to charge the capacitor is $t = Q / I$

The frequency output is then written as: $f = \frac{I}{Q} = \frac{I}{CV}$.

With the capacitor C being constant, the output frequency is then proportional to the current, hence proportional to the absolute temperature. Figure 9 shows the schematic of the Schmitt trigger. Sizing of the transistors are labeled on the schematic. The sizing was designed to achieve a hysteresis window to guarantee the safe operation of using MOS-capacitor. Simulation shows the hysteresis window is from 1.3 V to 3.6 V, which also validates the use of MOS-capacitor for its operation is in deep saturation. The simulation of the hysteresis window is shown in Figure 10.

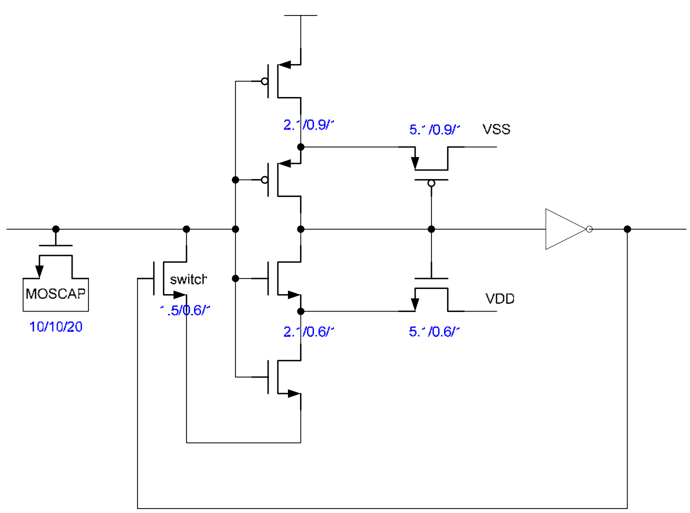

Figure 9 Schmitt trigger schematic

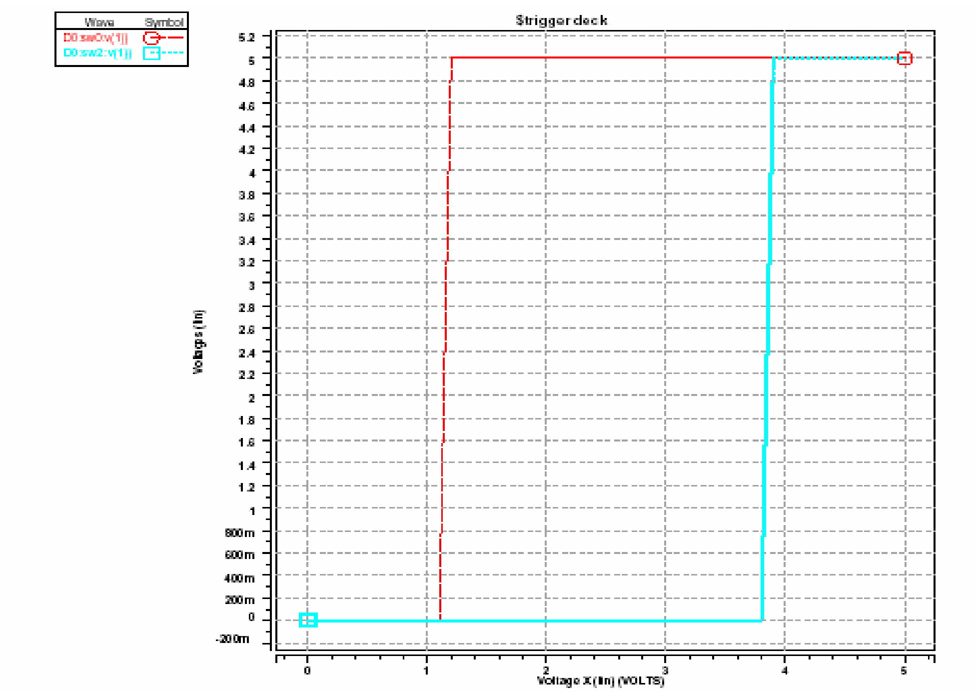

Figure 10 S-trigger hysteresis window simulation

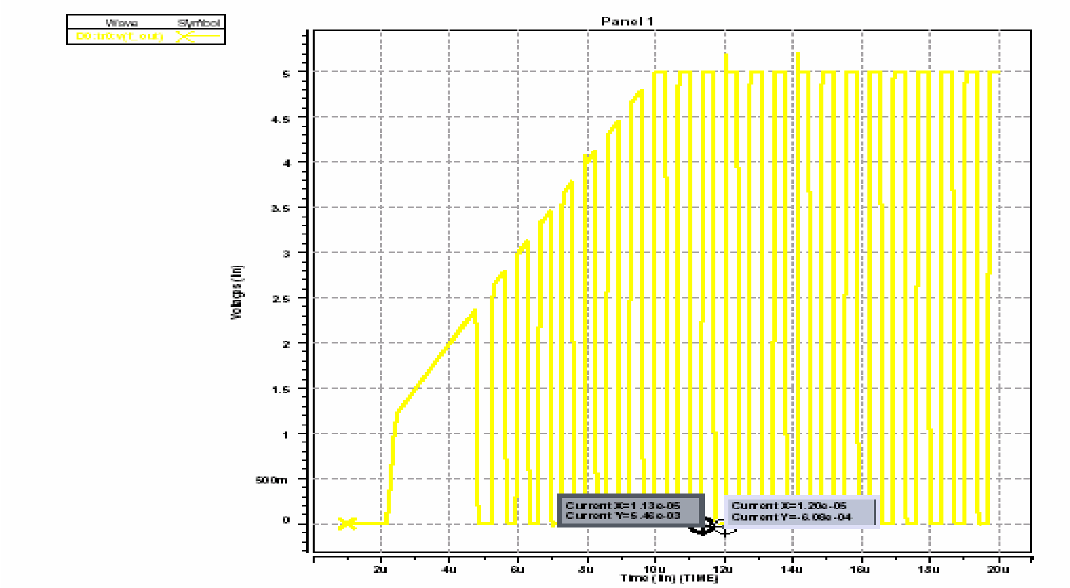

Figure 11 Frequency output at 100°C

4. Test results

The micro-luminometer and the temperature sensor were submitted together in two runs (T46TCA, T46TBZ) in order to acquire data from different wafers. The characterization experienced some ESD failure on some chip samples and in this section, some data are presented.

4.1. Micro-luminometer system

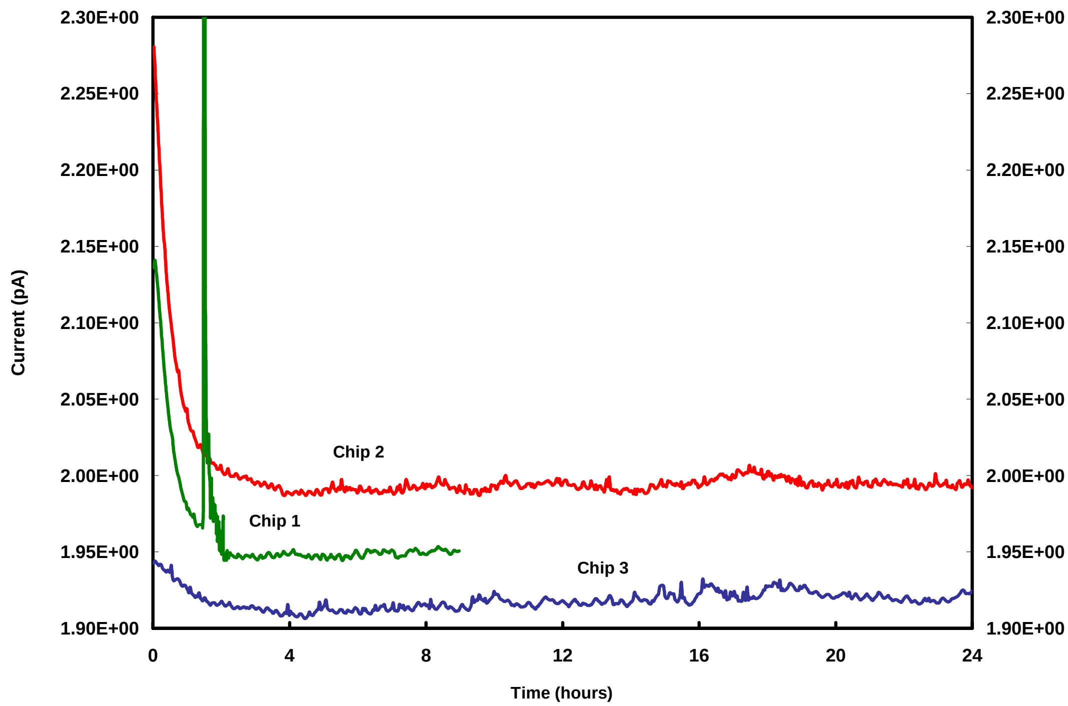

Figure 12 Micro-luminometer dark current

Figure 12 shows the characteristic leakage current, or dark current, associated with the on chip n-well/p-substrate photodiode. This current is present in the absence of any light and can be considered as a measurement offset. The dark current had a 4.5% variation (1.92pA – 2.01pA) over three chips using an estimated photodiode capacitance of 128pF.

4.2. *Temperature sensor*

Figure 13 shows the characteristics of output current vs. temperature from three different chips. For per degree change of temperature the average change of the output current is 0.22 µA, comparing to 0.134 µA in the simulation.

Figure 14 shows the characteristics of output frequency vs. temperature from three different chips. For per degree change of temperature, the average change of the output frequency is 3 to 4 kHz. Some idealities were shown in the test data, in which some were due to the chip failures where we attributed to insufficient on-chip ESD protection. Also, we found out the temperature sensor testing can be very sensitive to the test procedure. The thermal hysteresis of the diode can cause significant instability of the data.

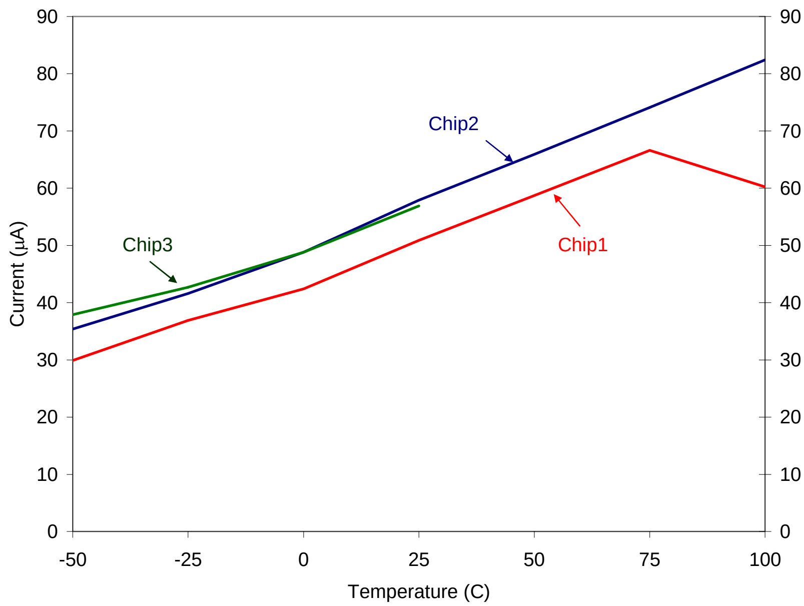

Figure 13 Output current vs. Temperature

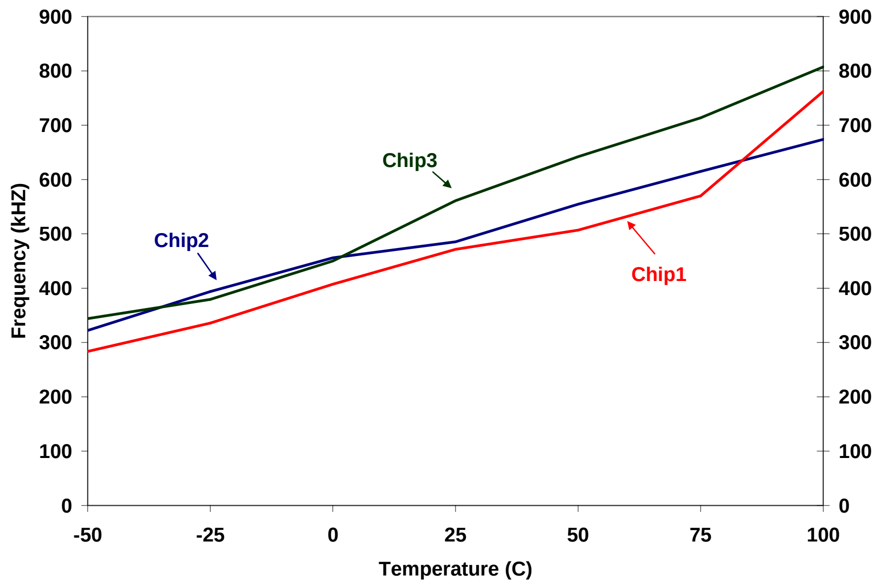

Figure 14 Output frequency vs. Temperature

5. Conclusion & Future Work

A micro-luminometer and a temperature sensor were designed, implemented, and tested on AMI 05 µm process. Lessons are learned for future revision.

Reference:

[1] W. Sansen, F. Eynde, and M.Steyaert, “A CMOS Temperature-compensated current reference,” *IEEE Journal of Solid-State Circuits,* Vol.23, No.3, June 1988